



PCCP

**Polymorphism and Phase Transitions in Na<sub>2</sub>U<sub>2</sub>O<sub>7</sub> from  
Density functional Perturbation Theory**

Journal:	<i>Physical Chemistry Chemical Physics</i>
Manuscript ID	CP-ART-03-2023-001222
Article Type:	Paper
Date Submitted by the Author:	17-Mar-2023
Complete List of Authors:	Weck, Philippe; Sandia National Laboratories Jove-colon, Carlos; Sandia National Laboratories Kim, Eunja; The University of Texas at El Paso

SCHOLARONE™  
Manuscripts



PCCP

ARTICLE

Received 00th January 20xx,

## Polymorphism and Phase Transitions in $\text{Na}_2\text{U}_2\text{O}_7$ from Density functional Perturbation Theory

Philippe F. Weck<sup>†a</sup>, Carlos F. Jové-Colón<sup>a</sup>, and Eunja Kim<sup>b</sup>

Accepted 00th January 20xx

DOI: 10.1039/x0xx00000x

www.rsc.org/

Polymorphism and phase transitions in sodium diuranate,  $\text{Na}_2\text{U}_2\text{O}_7$ , are investigated with density functional perturbation theory (DFPT). Thermal properties of crystalline  $\alpha$ -,  $\beta$ - and  $\gamma$ - $\text{Na}_2\text{U}_2\text{O}_7$  polymorphs are predicted from DFPT phonon calculations, i.e., the first time for the high-temperature  $\gamma$ - $\text{Na}_2\text{U}_2\text{O}_7$  phase ( $R\bar{3}m$  symmetry). The standard molar isochoric heat capacities predicted within the quasi-harmonic approximation are  $C_p^\circ(298.15\text{ K}) = 219.4$  and  $220.9\text{ J K}^{-1}\text{ mol}^{-1}$  for  $P2_1/a$   $\alpha$ - $\text{Na}_2\text{U}_2\text{O}_7$  and  $C2/m$   $\beta$ - $\text{Na}_2\text{U}_2\text{O}_7$ , respectively. Gibbs free energy calculations reveal that  $\alpha$ - $\text{Na}_2\text{U}_2\text{O}_7$  ( $P2_1/a$ ) and  $\beta$ - $\text{Na}_2\text{U}_2\text{O}_7$  ( $C2/m$ ) are almost energetically degenerate at low temperature, with  $\beta$ - $\text{Na}_2\text{U}_2\text{O}_7$  becoming slightly more stable than  $\alpha$ - $\text{Na}_2\text{U}_2\text{O}_7$  as temperature increases. These findings are consistent with XRD data showing a mixture of  $\alpha$  and  $\beta$  phases after cooling of  $\gamma$ - $\text{Na}_2\text{U}_2\text{O}_7$  to room temperature and the observation of a sluggish  $\alpha \rightarrow \beta$  phase transition above ca. 600 K. A recently observed  $\alpha$ - $\text{Na}_2\text{U}_2\text{O}_7$  structure with  $P2_1$  symmetry is also shown to be metastable at low temperature. Based on Gibbs free energy, no direct  $\beta \rightarrow \gamma$  solid-solid phase transition is predicted at high temperature, although some experiments reported the existence of such phase transition around 1348 K. This, along with recent experiments, suggests the occurrence of a multi-step process consisting of initial  $\beta$ -phase decomposition, followed by recrystallization into  $\gamma$ -phase as temperature increases.

### Introduction

Knowledge of the structure-thermodynamics relationships of secondary corrosion phases formed upon degradation and dissolution of  $\text{UO}_2$  spent nuclear fuel is crucial to reliably predict the behavior of radionuclides in geologic disposal environments for safety assessments. While the solubility and fate of actinides under typical environmental conditions have been investigated extensively,<sup>1,2,3</sup> comparatively less work has been dedicated to actinide chemistry and secondary phases formation under highly alkaline conditions. Such conditions can be found, for example, at the front- and back-end of the fuel cycle in Generation IV sodium-cooled fast reactors (SFR) envisioned for future commercial deployment. For this reason, there has been recently a growing interest in relative phase stability in the pseudo-ternary Na–U–O system in the context of SFR technology and safety<sup>4,5,6</sup>.

Highly alkaline conditions in the Na–U–O system can also occur in nuclear waste storage, e.g., at tank farms containing radioactive waste generated as a legacy by-product of nuclear weapons production. At some tank farms, PUREX-process alkaline sludge has been stored, as well as alkaline supernatant liquid wastes from the REDOX and PUREX processes<sup>7</sup>. In several instances, NaOH was added to highly acidic radioactive waste solutions, generated from the processing of irradiated nuclear fuel materials, to produce waste products compatible with

carbon steel storage tanks<sup>8</sup>. As a result of NaOH addition, an insoluble sludge waste was formed by precipitation of base-insoluble oxides and hydroxides of various metals. Waste dewatering by evaporation is often necessary because of limited tank farm capacity. However, dewatering leads to saturation of the solution in certain sodium salts, followed by crystallization of various sodium-containing solid phases after cooling in post-evaporation receipt tanks.

A study of tank waste samples to determine uranium and plutonium solubility limits revealed that the primary solid phase of uranium observed in equilibrium with the tank waste supernate solutions was the mineral clarkeite<sup>9</sup>, with an ideal chemical formula of  $\text{Na}[(\text{UO}_2)\text{O}(\text{OH})]\cdot(\text{H}_2\text{O})_{0.1}$  at hydroxide concentrations  $< 3.9\text{M}$ , and sodium diuranate,  $\text{Na}_2\text{U}_2\text{O}_7$ , at much higher hydroxide concentration<sup>8</sup> ( $> 8.7\text{M}$ ). This observation is consistent with the expectation that uranium exists as the hexavalent uranyl ion  $\text{UO}_2^{2+}$  under tank waste conditions<sup>8</sup>, as well as with the prediction that  $\text{Na}_2\text{U}_2\text{O}_7$  and clarkeite should be the dominant uranium solid phases under alkaline conditions<sup>10</sup>. Understanding the complex relationships between crystal structures and thermodynamic stability in the sodium uranate system is crucial to avoid the inadvertent precipitation, crystallization, and accumulation of uranium-bearing materials in process vessels and transfer pipes at nuclear waste storage tank farms. However, a clear consensus on the structures and relative thermal stabilities of some sodium uranate polymorphs has yet to be reached.

The early structural information on  $\text{Na}_2\text{U}_2\text{O}_7$  was reviewed by Keller<sup>11</sup>. Three polymorphs,  $\alpha$ -,  $\beta$ - and  $\gamma$ - $\text{Na}_2\text{U}_2\text{O}_7$ , were identified experimentally. Powder samples of  $\text{Na}_2\text{U}_2\text{O}_7$  were

<sup>a</sup> Sandia National Laboratories, Albuquerque, NM 87185, USA.

<sup>b</sup> Department of Physics, The University of Texas at El Paso, El Paso, TX 79902, USA.

<sup>†</sup> E-mail: pfwreck@sandia.gov.

initially described as adopting an isotopic lacunar structure of  $\text{CaUO}_4$ , crystallizing in the rhombohedral ditrigonal scalenohedral space group  $R\bar{3}m$  (IT No. 166,  $Z = 3/2$ )<sup>12</sup> or in a hexagonal unit cell<sup>13</sup>, and later in the monoclinic system<sup>14</sup>. The first pure single crystal of the high-temperature  $\gamma\text{-Na}_2\text{U}_2\text{O}_7$  polymorph was synthesized at 1200 °C by Gasperin<sup>15</sup> using a mixture of  $\text{U}_3\text{O}_8$  and  $\text{Na}_2\text{CO}_3$  and was found after cooling to crystallize in the  $R\bar{3}m$  space group. Clarkeite, the only known naturally occurring, high-temperature uranate mineral, was also characterized as adopting the  $R\bar{3}m$  space group<sup>9</sup> (IT No. 166,  $Z = 3$ ). The thermodynamic properties of  $\text{Na}_2\text{U}_2\text{O}_7$  were studied experimentally by Cordfunke et al., along with polymorphism and reversible structural phase transitions at 638 K ( $\alpha\text{-Na}_2\text{U}_2\text{O}_7 \rightarrow \beta\text{-Na}_2\text{U}_2\text{O}_7$ ) and 1348 K ( $\beta\text{-Na}_2\text{U}_2\text{O}_7 \rightarrow \gamma\text{-Na}_2\text{U}_2\text{O}_7$ )<sup>14,16</sup>. To the best of our knowledge, no thermodynamic functions have been reported for  $\gamma\text{-Na}_2\text{U}_2\text{O}_7$ .<sup>4,16</sup> Using powder X-ray diffraction (XRD) data, Kovba<sup>17</sup> found that the room temperature  $\alpha\text{-Na}_2\text{U}_2\text{O}_7$  structure adopts the  $C2/m$  (IT No. 12) space group. However, based on XRD measurements, Smith and coworkers<sup>4</sup> later found that the room-temperature  $\alpha\text{-Na}_2\text{U}_2\text{O}_7$  crystallizes in the monoclinic space group  $P2_1$  (IT No. 4,  $Z = 2$ ), and is isostructural<sup>18,19</sup> with  $\text{Na}_2\text{Np}_2\text{O}_7$  and  $\text{K}_2\text{U}_2\text{O}_7$ . In contrast with the studies by Cordfunke et al., both XRD and differential scanning calorimetry (DSC) experiments by Smith et al.<sup>4</sup> did not show the existence of the  $\alpha \rightarrow \beta$  phase transition above 600 K.

Recently, the lower-temperature crystal structures of synthetic  $\alpha$ - and  $\beta\text{-Na}_2\text{U}_2\text{O}_7$  polymorphs were determined from neutron powder diffraction by Ijdo et al.<sup>5</sup> At 293 K,  $\alpha\text{-Na}_2\text{U}_2\text{O}_7$  was found to crystallize in a monoclinic unit cell, space group  $P2_1/a$  (IT No. 14,  $Z = 4$ ), instead of the proposed  $C2/m$  or  $P2_1$  space groups<sup>4,17</sup>. At 773K,  $\beta\text{-Na}_2\text{U}_2\text{O}_7$  was also characterized as monoclinic, with space group  $C2/m$  (IT No. 12,  $Z = 4$ ). Ijdo et al. conjectured that the  $C2/m$  symmetry assignment by Kovba<sup>17</sup> for the room-temperature phase of  $\text{Na}_2\text{U}_2\text{O}_7$  might be the result of insufficient annealing and occurrence of micro-twinning in the room-temperature sample characterized with XRD. This suggestion seems plausible owing to the slow kinetics of the  $\alpha\text{-Na}_2\text{U}_2\text{O}_7 \leftrightarrow \beta\text{-Na}_2\text{U}_2\text{O}_7$  reversible transformation<sup>5,16</sup>. In light of the findings by Ijdo et al.<sup>5</sup>, Smith and coworkers<sup>20</sup> reinvestigated polymorphism for  $\text{Na}_2\text{U}_2\text{O}_7$  and confirmed with XRD the existence of  $\alpha$ -,  $\beta$ - and  $\gamma\text{-Na}_2\text{U}_2\text{O}_7$ , along with  $\alpha \rightarrow \beta$  and  $\beta \rightarrow \gamma$  phase transitions at above  $\sim 600$  K and in the range 1223-1323 K, respectively. They also reported that after complete cooling to room temperature of what they expected to be either pure  $\beta\text{-Na}_2\text{U}_2\text{O}_7$  or  $\gamma\text{-Na}_2\text{U}_2\text{O}_7$ , the final XRD pattern always corresponded to a mixture of  $\alpha$  and  $\beta$  phases<sup>20</sup>. Given the above discussion, a clear understanding of the relationships between structures and relative thermodynamic stabilities of  $\text{Na}_2\text{U}_2\text{O}_7$  polymorphs is still missing.

In this study, the  $\alpha$ -,  $\beta$ - and  $\gamma\text{-Na}_2\text{U}_2\text{O}_7$  phases have been investigated using density functional theory (DFT), followed by density functional perturbation theory (DFPT) calculations to determine their phonon and thermodynamic properties, and relative phase stability and phase transitions. Details of our computational approach are given in the next section, followed by a complete analysis and discussion of our results.

## Computational Methods

First-principles calculations were carried out using spin-polarized density functional theory implemented in the Vienna Ab initio Simulation Package (VASP)<sup>21</sup>. The exchange-correlation energy was calculated within the generalized gradient approximation<sup>22</sup> (GGA), with the parameterization of Perdew, Burke, and Ernzerhof<sup>23</sup> (PBE). As shown in previous studies, standard GGA is sufficient to correctly describe crystal phases of the pseudo-ternary Na–U–O system<sup>6</sup>, unlike uranium(IV) oxide  $\text{UO}_2$  bulk, which requires an effective Hubbard parameter or self-interaction correction to account for strong on-site Coulomb repulsion between localized uranium  $5f$  electrons. Standard functionals such as the PBE or PW91 functionals were found in previous studies to accurately describe the structures and properties of uranium oxides and uranium compounds characterized experimentally.<sup>6,24,25,26,27,28,29,30,31,32</sup>

The interaction between valence electrons and ionic cores was described by the projector augmented wave (PAW) method.<sup>33,34</sup> The  $\text{U}(6s^2,6p^6,7s^2,5f^3,6d^1)$ ,  $\text{Na}(2s^2,2p^6,3s^1)$ , and  $\text{O}(2s^2,2p^4)$  electrons were treated explicitly as valence electrons in the Kohn-Sham (KS) equations and the remaining core electrons together with the nuclei were represented by PAW pseudopotentials. KS equations were solved using the blocked Davidson<sup>35</sup> iterative matrix diagonalization scheme followed by the residual vector minimization method. The plane-wave cutoff energy for the electronic wavefunctions was set to a value of 700 eV, ensuring the total energy of the system to be converged to within 1 meV/atom.

Ionic and cell relaxations by total-energy minimization of  $\text{Na}_2\text{Np}_2\text{O}_7$  periodic simulation cells were first conducted simultaneously, without symmetry constraint applied, using as starting geometries the latest crystal structures characterized experimentally by Ijdo et al.<sup>5</sup> for the  $\alpha$ -phase ( $P2_1/a$ ) and  $\beta$ -phase ( $C2/m$ ), by Smith and coworkers<sup>4</sup> for the  $\alpha$ -phase with  $P2_1$  symmetry, and by Gasperin<sup>15</sup> for the  $\gamma$ -phase ( $R\bar{3}m$ ). The Hellmann-Feynman forces acting on atoms with the cells were calculated with a convergence tolerance set to 0.01 eV/Å. The Brillouin zone (BZ) was sampled using the Monkhorst-Pack  $k$ -point scheme<sup>36</sup> with  $k$ -point meshes of  $3 \times 5 \times 5$  for the  $P2_1/a$   $\alpha$ -phase and  $\beta$ -phase,  $5 \times 5 \times 5$  for the  $P2_1$   $\alpha$ -phase, and  $5 \times 5 \times 3$  for the  $\gamma$ -phase.

Phonon properties were computed with the linear response method implemented in VASP, which uses DFPT to calculate forces. In these calculations, using the optimized structures obtained from total-energy minimization, successive relaxations with respect to Hellmann-Feynman forces were carried out with a convergence tolerance set to 0.001 eV/Å. Thermodynamic properties of  $\text{Na}_2\text{Np}_2\text{O}_7$  polymorphs were derived, within the quasi-harmonic approximation (QHA), from phonon frequencies predicted with DFPT, for several expanded and compressed states in the vicinity of the equilibrium crystal structures. Due to the close similarity between the  $P2_1/a$   $\alpha$ -phase and the  $\beta$ -phase, structural symmetry was systematically checked after optimization of compressed and expanded crystal structures.

## Results and discussion

### Crystal structures

Figure 1 shows the crystal unit cells of  $\alpha$ -,  $\beta$ -, and  $\gamma$ - $\text{Na}_2\text{U}_2\text{O}_7$  relaxed at 0 K using VASP at the GGA/PBE level of theory. The structural parameters of  $\alpha$ -,  $\beta$ -, and  $\gamma$ - $\text{Na}_2\text{U}_2\text{O}_7$  calculated in this study are summarized in Table 1, along with previous experimental and DFT results.

The optimized structure of  $\alpha$ - $\text{Na}_2\text{U}_2\text{O}_7$  crystallizing in a monoclinic unit cell, space group  $P2_1/a$  (IT No. 14,  $Z = 4$ ), has lattice parameters of  $a = 13.024 \text{ \AA}$ ,  $b = 7.850 \text{ \AA}$ ,  $c = 6.912 \text{ \AA}$  ( $b/a = 0.603$ ,  $c/a = 0.531$ ,  $V = 659.06 \text{ \AA}^3$ ), and  $\beta = 111.16^\circ$  (see Figure 1(a)). These values are in good agreement with the recent neutron scattering measurements of  $a = 12.7617(14) \text{ \AA}$ ,  $b = 7.8384(10) \text{ \AA}$ ,  $c = 6.8962(9) \text{ \AA}$  ( $b/a = 0.6142$ ,  $c/a = 0.5404$ ,  $V = 642.78 \text{ \AA}^3$ ), and  $\beta = 111.285(9)^\circ$  at 293 K by Ijdo et al.<sup>5</sup>, as well as with the parameters of  $a = 12.778(3) \text{ \AA}$ ,  $b = 7.823(3) \text{ \AA}$ ,  $c = 6.880(3) \text{ \AA}$  ( $b/a = 0.612$ ,  $c/a = 0.538$ ,  $V = 640.9 \text{ \AA}^3$ ), and  $\beta = 111.28(5)^\circ$  determined from XRD data at 303 K by Smith et al.<sup>20</sup> Previous DFT calculations by Smith et al.<sup>6</sup> using CASTEP with GGA/PBE predicted a larger unit cell, with lattice parameters of  $a = 13.1322 \text{ \AA}$ ,  $b = 7.8815 \text{ \AA}$ ,  $c = 6.9292 \text{ \AA}$  ( $b/a = 0.6002$ ,  $c/a = 0.5276$ ,  $V = 669.18 \text{ \AA}^3$ ), and  $\beta = 110.994^\circ$ . The predicted equilibrium cell volume in this study is  $\sim 2.5\%$  larger than the experimental estimate of Ijdo et al.<sup>5</sup> – although  $\sim 1.5\%$  smaller than the DFT estimate of Smith et al.<sup>6</sup> –, owing to the well-known tendency of GGA functionals to overestimate bond distances.

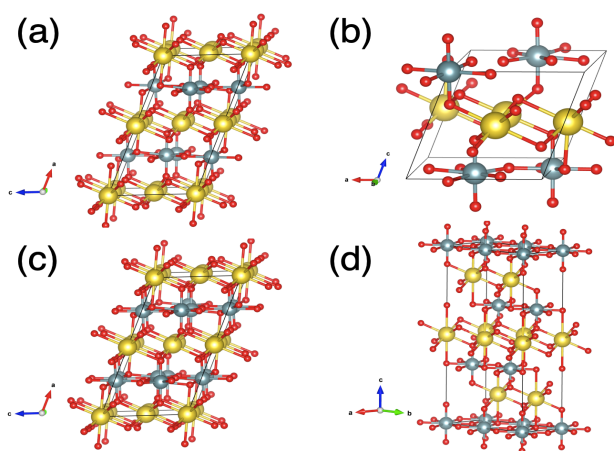


**Figure 1.** Crystal unit cells of (a)  $\alpha$ - $\text{Na}_2\text{U}_2\text{O}_7$  with  $P2_1/a$  symmetry (IT No. 14,  $Z = 4$ ), (b)  $\alpha$ - $\text{Na}_2\text{U}_2\text{O}_7$  with  $P2_1$  symmetry (IT No. 4,  $Z = 2$ ), (c)  $\beta$ - $\text{Na}_2\text{U}_2\text{O}_7$  with  $C2/m$  symmetry (IT No. 12,  $Z = 4$ ), and (d)  $\gamma$ - $\text{Na}_2\text{U}_2\text{O}_7$  with  $R\bar{3}m$  symmetry (IT No. 166,  $Z = 3$ ), relaxed with DFT at the GGA/PBE level of theory. Color legend: Na, yellow; O, red; U, teal.

The relaxed structure of  $\alpha$ - $\text{Na}_2\text{U}_2\text{O}_7$  adopting the monoclinic space group  $P2_1$  (IT No. 4,  $Z = 2$ ) exhibits lattice parameters of  $a = 6.908 \text{ \AA}$ ,  $b = 7.877 \text{ \AA}$ ,  $c = 6.504 \text{ \AA}$  ( $b/a = 1.140$ ,  $c/a = 0.942$ ,  $V = 331.44 \text{ \AA}^3$ ), and  $\beta = 110.53^\circ$  (Figure 1(b)), close to the room-temperature XRD values of  $a = 6.887(3) \text{ \AA}$ ,  $b = 7.844(3) \text{ \AA}$ ,  $c = 6.380(3) \text{ \AA}$  ( $b/a = 1.139$ ,  $c/a = 0.926$ ,  $321.16 \text{ \AA}^3$ ) and  $\beta = 111.29(5)^\circ$  measured by Smith and coworkers<sup>4</sup>. The computed unit-cell volume is  $\sim 3\%$  larger than XRD experiments.

**Table 1.** Structural parameters of  $\alpha$ -,  $\beta$ -, and  $\gamma$ - $\text{Na}_2\text{U}_2\text{O}_7$  unit cells.<sup>a</sup>

Phase	$\alpha$	$\alpha$	$\beta$	$\gamma$
Symmetry	$P2_1/a$	$P2_1$	$C2/m$	$R\bar{3}m$
IT No.	14	4	12	166
Z	4	2	4	3
$a(\text{\AA})$	<b>13.024</b> 12.7617 <sup>b</sup> 12.778 <sup>e</sup> 13.1322 <sup>f</sup>	<b>6.908</b> 6.887 <sup>c</sup>	<b>13.022</b> 12.933 <sup>b</sup> 12.946 <sup>e</sup> 13.125 <sup>f</sup>	<b>3.989</b> 3.911 <sup>d</sup> 3.987 <sup>e</sup>
$b(\text{\AA})$	<b>7.850</b> 7.8384 <sup>b</sup> 7.823 <sup>e</sup> 7.8815 <sup>f</sup>	<b>7.877</b> 7.844 <sup>c</sup>	<b>7.850</b> 7.887 <sup>b</sup> 7.894 <sup>e</sup> 7.881 <sup>f</sup>	<b>7.964</b> 7.822 <sup>d</sup> 7.974 <sup>e</sup>
$c(\text{\AA})$	<b>6.912</b> 6.8962 <sup>b</sup> 6.880 <sup>e</sup> 6.9292 <sup>f</sup>	<b>6.504</b> 6.380 <sup>c</sup>	<b>6.912</b> 6.9086 <sup>b</sup> 6.910 <sup>e</sup> 6.9291 <sup>f</sup>	<b>18.110</b> 17.857 <sup>d</sup> 18.491 <sup>e</sup>
$\beta(^\circ)$	<b>111.16</b> 111.285 <sup>b</sup> 111.28 <sup>e</sup> 110.994 <sup>f</sup>	<b>110.53</b> 111.29 <sup>c</sup>	<b>111.15</b> 110.816 <sup>b</sup> 110.87 <sup>e</sup> 110.967 <sup>f</sup>	<b>90.00</b> 90.00 <sup>d</sup> 90.00 <sup>e</sup>
$V(\text{\AA}^3)$	<b>659.06</b> 642.78 <sup>b</sup> 640.9 <sup>e</sup> 669.18 <sup>f</sup>	<b>331.44</b> 321.16 <sup>c</sup>	<b>659.04</b> 658.80 <sup>b</sup> 659.8 <sup>e</sup> 669.33 <sup>f</sup>	<b>497.97</b> 472.32 <sup>d</sup> 509.2 <sup>e</sup>

<sup>a</sup> Unit-cell parameters optimized in this study with DFT at 0 K at the GGA/PBE level are shown in bold font.

<sup>b</sup> Neutron data at 293 K for  $\alpha$  phase and at 773 K for  $\beta$  phase by Ijdo et al., 2015.

<sup>c</sup> XRD data by Smith et al., 2014.

<sup>d</sup> XRD data by Gasperin, 1986. The cell was doubled along the  $b$  axis for direct comparison with the  $Z=3$  cell used in present DFT calculations.

<sup>e</sup> XRD data at 303 K for  $\alpha$  phase, at 748 K for  $\beta$  phase, and at 1323 K for  $\gamma$  phase by Smith et al., 2015.

<sup>f</sup> DFT at 0 K with CASTEP at the GGA/PBE level by Smith et al., 2017.

As shown in Figure 1(c), the monoclinic  $\beta$ - $\text{Na}_2\text{U}_2\text{O}_7$  polymorph with  $C2/m$  symmetry (IT No. 12,  $Z = 4$ ) is very similar overall to the  $P2_1/a$   $\alpha$ - $\text{Na}_2\text{U}_2\text{O}_7$  structure, and its optimized lattice parameters are  $a = 13.022 \text{ \AA}$ ,  $b = 7.850 \text{ \AA}$ ,  $c = 6.912 \text{ \AA}$  ( $b/a = 0.603$ ,  $c/a = 0.531$ ) and  $\beta = 111.15^\circ$ , which closely reproduce the XRD values of  $a = 12.933(1) \text{ \AA}$ ,  $b = 7.887(1) \text{ \AA}$ ,  $c = 6.9086(8) \text{ \AA}$  ( $b/a = 0.610$ ,  $c/a = 0.534$ ) and  $\beta = 110.816(10)^\circ$  reported at 773 K by Ijdo et al.<sup>5</sup> Similar to the case of  $P2_1/a$   $\alpha$ - $\text{Na}_2\text{U}_2\text{O}_7$  discussed above, DFT calculations for  $\beta$ - $\text{Na}_2\text{U}_2\text{O}_7$  by Smith et al.<sup>6</sup> with CASTEP/GGA/PBE predicted a systematically larger unit cell, with lattice parameters of  $a = 13.125 \text{ \AA}$ ,  $b = 7.881 \text{ \AA}$ ,  $c = 6.9291 \text{ \AA}$  ( $b/a = 0.6002$ ,  $c/a = 0.5276$ ,  $V = 669.33 \text{ \AA}^3$ ), and  $\beta = 110.967^\circ$ . As discussed by Ijdo et al.<sup>5</sup>, the  $\alpha$ - and  $\beta$ - $\text{Na}_2\text{U}_2\text{O}_7$  structures, which both consist of nearly closed-packed cubic Na and U layers, differ essentially by the higher degree of tilting and deformation of the corner-linked U-O coordination octahedra and edged-linked U-O pentagonal bipyramids in  $\alpha$ -phase compared to  $\beta$ -phase.

Finally, the relaxed structure of  $\gamma$ - $\text{Na}_2\text{U}_2\text{O}_7$  with  $R\bar{3}m$  symmetry (IT No. 166,  $Z = 3$ ) has predicted lattice parameters of

$a = 3.989 \text{ \AA}$  and  $c = 18.110 \text{ \AA}$  ( $c/a = 4.540$ ), and  $\gamma = 120.06^\circ$  (see Figure 1(d)), in agreement with the single crystal characterized by Gasperin<sup>15</sup> with lattice parameters of  $a = 3.911(3) \text{ \AA}$  and  $c = 17.857(5) \text{ \AA}$  ( $c/a = 4.565$ ), and very similar to the natural clarkeite sample analyzed by Finch and Ewing<sup>9</sup>, featuring lattice parameters of  $a = 3.954(4) \text{ \AA}$  and  $c = 17.73(1) \text{ \AA}$  ( $c/a = 4.484$ ). The possible presence of residual  $\text{H}_2\text{O}$  in this clarkeite sample appears to slightly elongate the crystal along the  $a$ -axis and shorten the crystal along the  $c$  axis compared to the anhydrous, single-crystal  $\gamma\text{-Na}_2\text{U}_2\text{O}_7$  sample synthesized by Gasperin and modeled in this study.

### Thermodynamic Properties

Analysis from sets of phonon calculations in the vicinity of the computed equilibrium crystal structures of  $\text{Na}_2\text{U}_2\text{O}_7$  polymorphs was carried out to derive their thermal properties at ambient pressure, in steps of 10 K. The QHA utilized here introduces a volume dependence of phonon frequencies as a part of anharmonic effect.<sup>37</sup> The Gibbs free energy is defined at a constant pressure by the transformation:

$$G(T, p) = \min_V [U(V) + F_{\text{phonon}}(T; V) + pV],$$

where  $\min_V$  [function of  $V$ ] corresponds to a unique minimum of the expression between brackets with respect to the volume  $V$ ,  $U(V)$  is the total energy of the system, and  $p$  is the pressure applied.  $U(V)$  and  $F_{\text{phonon}}(T; V)$  were calculated and the thermodynamic functions of the right-hand sides of the equation above were fitted to the integral forms of the Vinet equation of state (EOS). The phonon contribution to the Helmholtz free energy at constant volume  $V$ , was calculated using the following formula:

$$F_{\text{phonon}}(T) = \frac{1}{2} \sum \hbar\omega + k_B T \sum \ln[1 - e^{-\beta\hbar\omega}],$$

where  $\hbar$  is the reduced Planck constant,  $\hbar\omega$  is the energy of a single phonon with angular frequency  $\omega$ ,  $k_B$  is the Boltzmann constant,  $T$  is the temperature of the system, and  $\beta = (k_B T)^{-1}$ .

The thermal evolutions of the Gibbs free energy of  $\alpha\text{-Na}_2\text{U}_2\text{O}_7$  with  $P2_1/a$  and  $P2_1$  symmetries,  $\beta\text{-Na}_2\text{U}_2\text{O}_7$  with  $C2/m$  symmetry, and  $\gamma\text{-Na}_2\text{U}_2\text{O}_7$  with  $R\bar{3}m$  symmetry predicted using DFPT/QHA are displayed in Figure 2. Calculations show that  $\alpha\text{-Na}_2\text{U}_2\text{O}_7$  with  $P2_1/a$  symmetry and  $\beta\text{-Na}_2\text{U}_2\text{O}_7$  are essentially energetically-degenerate at low temperature, with Gibbs energy differences of  $\sim 1 \text{ meV}$ . These findings are in-line with observation by Smith et al. that heating the room-temperature  $\text{Na}_2\text{U}_2\text{O}_7$  phase to above 1100 K, followed by cooling to low temperature, always resulted in a  $\alpha+\beta$  mixture, instead of pure  $\alpha$ , or  $\beta$ , or  $\gamma$  phase<sup>20</sup>. As the temperature increases,  $\beta\text{-Na}_2\text{U}_2\text{O}_7$  tends to become slightly more stable than  $P2_1/a$   $\alpha\text{-Na}_2\text{U}_2\text{O}_7$ , which is consistent with the observation of a  $\alpha \rightarrow \beta$  phase transition at above  $\sim 600 \text{ K}$  by Smith and coworkers<sup>20</sup> and by Cordfunke et al.<sup>14,16</sup> Since the energy difference between both phases is only  $\sim 0.015 \text{ eV}$  at 600 K, this  $\alpha \rightarrow \beta$  phase transition is predicted to be rather sluggish; this finding is in agreement with the experimental characterization by Kovba<sup>17</sup>, and by Cordfunke

et al.<sup>16</sup>, and by Ijdo et al.<sup>5</sup>, who all reported slow kinetics for the  $\alpha \rightarrow \beta$  phase transition. Due to minute differences between the  $\alpha$  and  $\beta$  phases, this transition is particularly difficult to detect with XRD or DSC techniques, as described by Smith et al.<sup>4</sup> In addition, calculations show that at low temperature the  $\alpha\text{-Na}_2\text{U}_2\text{O}_7$  structure adopting the monoclinic space group  $P2_1$  reported by Smith and coworkers<sup>4</sup> is only slightly less energetically favorable than the  $\alpha\text{-Na}_2\text{U}_2\text{O}_7$  with  $P2_1/a$  symmetry; the difference in Gibbs free energy between  $\alpha\text{-Na}_2\text{U}_2\text{O}_7$  with  $P2_1/a$  and  $P2_1$  symmetries is less than  $\sim 0.04 \text{ eV}$  near the zero-temperature limit. Therefore, it can be inferred that the metastable  $P2_1$   $\alpha\text{-Na}_2\text{U}_2\text{O}_7$  characterized by Smith et al. might eventually decay into  $P2_1/a$   $\alpha\text{-Na}_2\text{U}_2\text{O}_7$  or a mixture of  $P2_1/a$   $\alpha\text{-Na}_2\text{U}_2\text{O}_7$  and  $\beta\text{-Na}_2\text{U}_2\text{O}_7$  phases.

Similarly, calculations show that the pure  $\gamma\text{-Na}_2\text{U}_2\text{O}_7$  phase with  $R\bar{3}m$  symmetry is metastable at low temperature, with respect to the  $P2_1/a$   $\alpha\text{-Na}_2\text{U}_2\text{O}_7$  and  $\beta\text{-Na}_2\text{U}_2\text{O}_7$  phases. This explains why pure  $\gamma\text{-Na}_2\text{U}_2\text{O}_7$  phase synthesized at high temperature (i.e., above  $\sim 1473 \text{ K}$  by Gasperin<sup>15</sup>) has to be rapidly quenched to room temperature for crystallographic characterization. As reported by Smith et al.<sup>20</sup>, gradual cooling of  $\gamma\text{-Na}_2\text{U}_2\text{O}_7$  to room temperature of what was expected to be either pure  $\beta\text{-Na}_2\text{U}_2\text{O}_7$  or  $\gamma\text{-Na}_2\text{U}_2\text{O}_7$ , resulted instead in a mixture of  $\alpha$  and  $\beta$  phases.

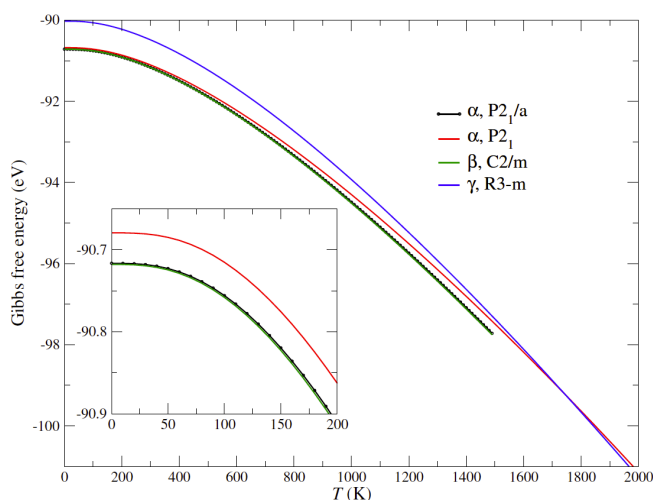
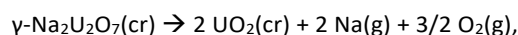


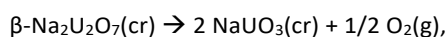
**Figure 2.** Variations of the Gibbs free energy of  $\alpha\text{-Na}_2\text{U}_2\text{O}_7$  with  $P2_1/a$  and  $P2_1$  symmetries,  $\beta\text{-Na}_2\text{U}_2\text{O}_7$  with  $C2/m$  symmetry, and  $\gamma\text{-Na}_2\text{U}_2\text{O}_7$  with  $R\bar{3}m$  symmetry computed with DFPT at the GGA/PBE level, within the QHA approximation at ambient pressure. *Inset:* close-up of the Gibbs free energy in the 0-200 K temperature range.

Although early experimental investigations reported the existence of a  $\beta\text{-Na}_2\text{U}_2\text{O}_7 \rightarrow \gamma\text{-Na}_2\text{U}_2\text{O}_7$  phase transition at 1348 K<sup>14,16</sup>, which was recently observed with XRD to be in the range 1223-1323 K by Smith and coworkers<sup>20</sup>, the present DFT calculations using pure, stoichiometric  $\beta\text{-Na}_2\text{U}_2\text{O}_7$  and  $\gamma\text{-Na}_2\text{U}_2\text{O}_7$  phases do not lend support to this interpretation. As depicted in Figure 2, the Gibbs free energy curve for the  $\beta\text{-Na}_2\text{U}_2\text{O}_7$  phase does not cross that of the  $\gamma\text{-Na}_2\text{U}_2\text{O}_7$  phase, therefore no direct temperature-driven  $\beta\text{-Na}_2\text{U}_2\text{O}_7 \rightarrow \gamma\text{-Na}_2\text{U}_2\text{O}_7$  solid-solid phase transition is expected to occur at high temperature. Similar to  $\beta\text{-Na}_2\text{U}_2\text{O}_7$ , the Gibbs free energy curve

of  $P2_1/a$   $\alpha$ - $\text{Na}_2\text{U}_2\text{O}_7$  does not intersect that of  $\gamma$ - $\text{Na}_2\text{U}_2\text{O}_7$ , thus eliminating the possibility of  $\alpha$ - $\text{Na}_2\text{U}_2\text{O}_7 \rightarrow \gamma$ - $\text{Na}_2\text{U}_2\text{O}_7$  solid-solid phase transition. In addition, although the Gibbs free energy curves of the  $\gamma$ - $\text{Na}_2\text{U}_2\text{O}_7$  phase and the metastable  $P2_1$   $\alpha$ - $\text{Na}_2\text{U}_2\text{O}_7$  phase do cross at  $\sim 1743$  K (Figure 2), experiments by Smith et al.<sup>6,20</sup> indicated that  $\gamma$ - $\text{Na}_2\text{U}_2\text{O}_7$  is completely decomposed around  $\sim 1620$  K according to the reaction:



with further vaporization of crystalline  $\text{UO}_2$  product occurring above  $\sim 1755$  K. Therefore, this rules out the occurrence of a possible interconversion between the metastable  $P2_1$   $\alpha$ - $\text{Na}_2\text{U}_2\text{O}_7$  phase and  $\gamma$ - $\text{Na}_2\text{U}_2\text{O}_7$  at high temperature and other mechanisms might be at play in the observed  $\beta$ - $\text{Na}_2\text{U}_2\text{O}_7 \rightarrow \gamma$ - $\text{Na}_2\text{U}_2\text{O}_7$  phase transition. Actual XRD characterization by Smith et al.<sup>4</sup> suggests that  $\beta$ - $\text{Na}_2\text{U}_2\text{O}_7$  starts decomposing at  $\sim 873$  K according to the reaction:



with the complete disappearance of  $\beta$ - $\text{Na}_2\text{U}_2\text{O}_7$  at 973 K. In turn, at 1073 K,  $\text{UO}_2(\text{cr})$  was observed<sup>4</sup> to form upon decomposition of  $\text{NaUO}_3(\text{cr})$  following the reaction:



where the  $\gamma$ - $\text{Na}_2\text{U}_2\text{O}_7$  product fully disappears by  $\sim 1620$  K, as discussed above. Evidence of  $\gamma$ - $\text{Na}_2\text{U}_2\text{O}_7(\text{cr})$  and  $\text{UO}_2(\text{cr})$  formation as products of  $\text{NaUO}_3(\text{cr})$  decomposition was later refined to the temperature range 1273-1373 K by Smith et al.<sup>20</sup> Based on these experimental observations,  $\beta$ - $\text{Na}_2\text{U}_2\text{O}_7$  (and  $\alpha$ - $\text{Na}_2\text{U}_2\text{O}_7$ ) is not expected to be stable above  $\sim 973$  K, and  $\gamma$ - $\text{Na}_2\text{U}_2\text{O}_7$  can be considered stable only in the range  $\sim 1073$ - $1620$  K. Therefore, in the remainder of this study, thermodynamic properties of the  $\text{Na}_2\text{U}_2\text{O}_7$  polymorphs will only be discussed in their respective stability ranges.

For all the  $\text{Na}_2\text{U}_2\text{O}_7$  polymorphs, the isobaric heat capacity at ambient pressure versus temperature was also derived as the second derivative of the Gibbs free energy with respect to  $T$ , i.e.:

$$C_p(T, p) = -T \frac{\partial^2 G(T, p)}{\partial T^2}.$$

Figure 3 shows the thermal variations of the molar isobaric heat capacity,  $C_p$ , of  $\alpha$ - $\text{Na}_2\text{U}_2\text{O}_7$  with  $P2_1/a$  and  $P2_1$  symmetries,  $\beta$ - $\text{Na}_2\text{U}_2\text{O}_7$  with  $C2/m$  symmetry, and  $\gamma$ - $\text{Na}_2\text{U}_2\text{O}_7$  with  $R\bar{3}m$  symmetry predicted in this study with DFPT, within the QHA approximation. For comparison, the low-temperature (5-350 K) molar isobaric heat capacity measured by Cordfunke et al.<sup>16</sup> using adiabatic calorimetry (AC) and the values derived from enthalpy increments (EI) of  $\alpha$ - $\text{Na}_2\text{U}_2\text{O}_7$  (390-558 K) and  $\beta$ - $\text{Na}_2\text{U}_2\text{O}_7$  (680-926 K) determined by drop calorimetry are depicted in Figure 3. Also shown are the DFT results at 298.15 K by Smith and coworkers<sup>6</sup> using the CASTEP code for  $\alpha$ - $\text{Na}_2\text{U}_2\text{O}_7$  ( $P2_1/a$ ) and  $\beta$ - $\text{Na}_2\text{U}_2\text{O}_7$  ( $C2/m$ ). At low temperature, the  $C_p$  values computed here for  $P2_1$   $\alpha$ - $\text{Na}_2\text{U}_2\text{O}_7$  are systematically

much smaller than the corresponding predictions for  $P2_1/a$   $\alpha$  and  $\beta$  polymorph structures, especially above  $\sim 200$  K, although calculated  $C_p$  values for  $\alpha$ - and  $\beta$ - $\text{Na}_2\text{U}_2\text{O}_7$  remain smaller than calorimetric data by Cordfunke and coworkers<sup>16</sup>. The experimental reference standard molar isochoric heat capacity measured using AC by Cordfunke et al. is  $C_p^\circ(298.15 \text{ K}) = 227.26 \text{ J K}^{-1} \text{ mol}^{-1}$ , while the values predicted in this study are  $212.0 \text{ J K}^{-1} \text{ mol}^{-1}$  (-6.7%),  $219.4 \text{ J K}^{-1} \text{ mol}^{-1}$  (-3.4%), and  $220.9 \text{ J K}^{-1} \text{ mol}^{-1}$  (-2.8%) for  $P2_1$   $\alpha$ - $\text{Na}_2\text{U}_2\text{O}_7$ ,  $P2_1/a$   $\alpha$ - $\text{Na}_2\text{U}_2\text{O}_7$ , and  $C2/m$   $\beta$ - $\text{Na}_2\text{U}_2\text{O}_7$ , respectively. Let us note that, based on the results and discussion of Figure 2, it can be inferred that the calorimetric data by Cordfunke et al. correspond to an actual mixture of  $\alpha$ - $\text{Na}_2\text{U}_2\text{O}_7$  ( $P2_1/a$ ) and  $\beta$ - $\text{Na}_2\text{U}_2\text{O}_7$  ( $C2/m$ ), instead of a pure  $\alpha$ - $\text{Na}_2\text{U}_2\text{O}_7$  phase as stated. In contrast, the  $C_p^\circ$  values predicted by Smith and coworkers<sup>6</sup> using a Debye-type model are  $229.5 \text{ J K}^{-1} \text{ mol}^{-1}$  for  $\alpha$ - $\text{Na}_2\text{U}_2\text{O}_7$  ( $P2_1/a$ ) and  $230.6 \text{ J K}^{-1} \text{ mol}^{-1}$  for  $\beta$ - $\text{Na}_2\text{U}_2\text{O}_7$  ( $C2/m$ ), i.e., +1.0% and +1.5% larger, respectively, than the calorimetric value. These larger values likely stem from the larger crystal cells utilized in simulations by Smith et al., up to 4% larger than the experimental volume for  $P2_1/a$   $\alpha$ - $\text{Na}_2\text{U}_2\text{O}_7$ . In addition, as mentioned by Smith et al.<sup>6</sup>, it is worth noting that the values for the enthalpy increments of  $\beta$ - $\text{Na}_2\text{U}_2\text{O}_7$  by Cordfunke and coworkers<sup>16</sup> could not be fitted reliably as the thermodynamic parameters at 298.15 K and at the transition temperature were not determined<sup>38</sup>. This might explain to some extent the larger discrepancies between the present DFPT results and data from EI measurements in the temperature ranges 390-558 K ( $P2_1/a$   $\alpha$ - $\text{Na}_2\text{U}_2\text{O}_7$ ) and 680-926 K ( $\beta$ - $\text{Na}_2\text{U}_2\text{O}_7$ ).

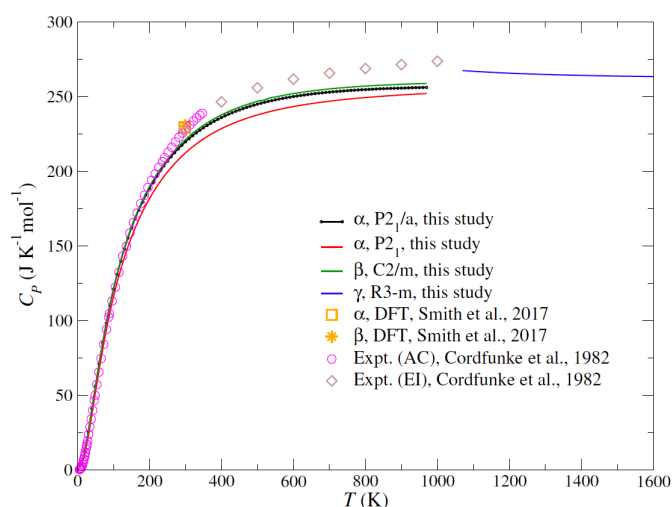


**Figure 3.** Thermal evolution of the molar isobaric heat capacity,  $C_p$ , of  $\alpha$ - $\text{Na}_2\text{U}_2\text{O}_7$  with  $P2_1/a$  and  $P2_1$  symmetries,  $\beta$ - $\text{Na}_2\text{U}_2\text{O}_7$  with  $C2/m$  symmetry, and  $\gamma$ - $\text{Na}_2\text{U}_2\text{O}_7$  with  $R\bar{3}m$  symmetry computed with DFPT at the GGA/PBE level at ambient pressure. The experimental values of the molar isobaric heat capacity measured by Cordfunke et al. (1982) from adiabatic calorimetry (AC) and enthalpy increments (EI), and the DFT  $C_p^\circ$  results by Smith and coworkers (Smith et al., 2017) for  $\alpha$ - $\text{Na}_2\text{U}_2\text{O}_7$  ( $P2_1/a$ ) and  $\beta$ - $\text{Na}_2\text{U}_2\text{O}_7$  ( $C2/m$ ) are also displayed for comparison.

The predicted molar isochoric heat capacity for  $\gamma$ - $\text{Na}_2\text{U}_2\text{O}_7$  varies between 263.43 and 267.51  $\text{J K}^{-1} \text{ mol}^{-1}$  in the 1070-1620 K temperature range, in close proximity to the Dulong-Petit asymptotic value of  $C_p = n3R = 274.38 \text{ J K}^{-1} \text{ mol}^{-1}$ , where  $n$  is the

number of atoms per formula-unit and  $R$  is the universal gas constant. While, to the best of our knowledge, no thermodynamic functions have been reported for  $\gamma$ - $\text{Na}_2\text{U}_2\text{O}_7$ <sup>4,16</sup>, the value reported by Cordfunke et al.<sup>16</sup> for  $\beta$ - $\text{Na}_2\text{U}_2\text{O}_7$  at 900 K is 271.50 J K<sup>-1</sup> mol<sup>-1</sup>, very close to present predictions for  $\gamma$ - $\text{Na}_2\text{U}_2\text{O}_7$  at higher temperature. Although shown in Figure 3, the value of 273.76 J K<sup>-1</sup> mol<sup>-1</sup> at 1000 K extrapolated by Cordfunke et al.<sup>16</sup> for  $\beta$ - $\text{Na}_2\text{U}_2\text{O}_7$  can probably be discarded since  $\beta$ - $\text{Na}_2\text{U}_2\text{O}_7$  starts decomposing into  $\text{NaUO}_3$  and  $\text{O}_2$  around 873 K and fully disappears above 973 K, as discussed above.

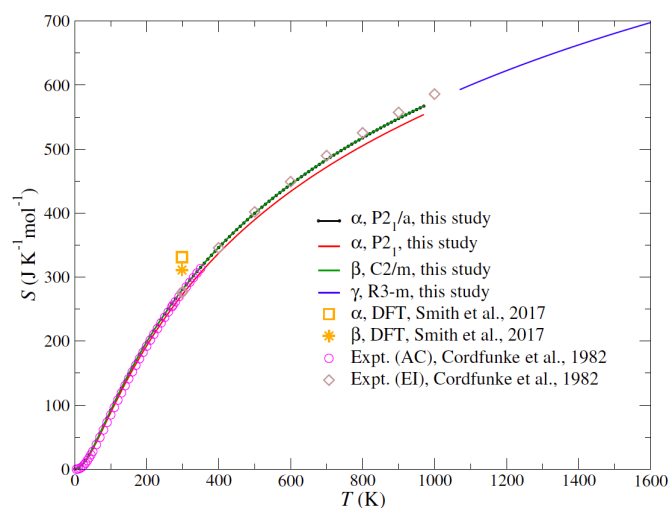


**Figure 4.** Thermal evolution of the molar entropy of  $\alpha$ - $\text{Na}_2\text{U}_2\text{O}_7$  with  $P2_1/a$  and  $P2_1$  symmetries,  $\beta$ - $\text{Na}_2\text{U}_2\text{O}_7$  with  $C2/m$  symmetry, and  $\gamma$ - $\text{Na}_2\text{U}_2\text{O}_7$  with R-3m symmetry computed with DFPT at the GGA/PBE level at ambient pressure. The experimental values of the molar entropy derived by Cordfunke et al. (1982) from adiabatic calorimetry (AC) and enthalpy increments (EI), and the DFT  $S^0$  results by Smith and coworkers (Smith et al., 2017) for  $\alpha$ - $\text{Na}_2\text{U}_2\text{O}_7$  ( $P2_1/a$ ) and  $\beta$ - $\text{Na}_2\text{U}_2\text{O}_7$  ( $C2/m$ ) are also displayed for comparison.

For each  $\text{Na}_2\text{U}_2\text{O}_7$  polymorph, the thermal evolution of the molar entropy was computed at constant equilibrium volume and ambient pressure, in the polymorphs respective thermal stability ranges, using the expression:

$$S(T) = -k_B \sum \ln[1 - e^{-\beta\hbar\omega}] - \frac{1}{T} \sum \frac{\hbar\omega}{e^{\beta\hbar\omega} - 1}$$

with all variables and constants as defined earlier. As shown in Figure 4, very good agreement is obtained between DFPT results in this study for  $P2_1/a$   $\alpha$ - and  $\beta$ -polymorph structures and experimental values of the molar entropy derived by Cordfunke and coworkers<sup>16</sup> from AC and EI measurements. In particular, the experimental reference standard molar entropy  $S^0 = 275.86$  J K<sup>-1</sup> mol<sup>-1</sup> derived by Cordfunke et al.<sup>16</sup> from AC measurements is close to the present DFPT values of 279.6 J K<sup>-1</sup> mol<sup>-1</sup> for  $P2_1/a$   $\alpha$ - $\text{Na}_2\text{U}_2\text{O}_7$  (+1.3%) and 279.8 J K<sup>-1</sup> mol<sup>-1</sup> for  $\beta$ - $\text{Na}_2\text{U}_2\text{O}_7$  (+1.4%), while the corresponding value for the candidate phase  $P2_1$   $\alpha$ - $\text{Na}_2\text{U}_2\text{O}_7$  is 272.1 J K<sup>-1</sup> mol<sup>-1</sup> (-1.4%). The values predicted by Smith and coworkers<sup>6</sup> using a Debye-type model are significantly larger than AC experiment, i.e., 331.3 J K<sup>-1</sup> mol<sup>-1</sup> for  $P2_1/a$   $\alpha$ - $\text{Na}_2\text{U}_2\text{O}_7$  (+20.1%) and 311.1 J K<sup>-1</sup> mol<sup>-1</sup> for

$\beta$ - $\text{Na}_2\text{U}_2\text{O}_7$  (+12.8%). The thermal evolution of  $S$  predicted here up to  $\sim 1600$  K for  $\gamma$ - $\text{Na}_2\text{U}_2\text{O}_7$  does not show any significant discontinuity with values calculated for  $\alpha$ - and  $\beta$ - $\text{Na}_2\text{U}_2\text{O}_7$  at lower temperature.

To derive the enthalpy function,  $(H_T - H_{298.15}) \cdot T^{-1}$ , and the Gibbs energy function,  $-(G_T - H_{298.15}) \cdot T^{-1}$ , the thermal evolution of the isobaric heat capacity calculated from DFPT for each  $\text{Na}_2\text{U}_2\text{O}_7$  polymorph was fitted using nonlinear least-squares regression to a Haas-Fisher-type polynomial:

$$C_p(T) = a + bT + cT^{-2} + dT^{-0.5} + eT^2,$$

The optimized polynomial coefficients for  $\alpha$ -,  $\beta$ - and  $\gamma$ - $\text{Na}_2\text{U}_2\text{O}_7$  are summarized in Table 2.

**Table 2.** Coefficients of the Haas-Fisher-type heat capacity polynomial  $C_p(T)$  for  $\alpha$ -,  $\beta$ - and  $\gamma$ - $\text{Na}_2\text{U}_2\text{O}_7$ . The ranges of validity of the fits are 100–970 K for  $\alpha$ - and  $\beta$ - $\text{Na}_2\text{U}_2\text{O}_7$ , and 1070–1620 K for  $\gamma$ - $\text{Na}_2\text{U}_2\text{O}_7$ .

Phase	$a \times 10^2$ ( $T^0$ )	$b \times 10^{-1}$ ( $T$ )	$c \times 10^5$ ( $T^{-2}$ )	$d \times 10^3$ ( $T^{-0.5}$ )	$e \times 10^{-5}$ ( $T^2$ )	SSD <sup>a</sup>
$\alpha$ $P2_1/a$	4.5627	-1.237	3.4728923	-3.57685	3.66	0.71
$\alpha$ $P2_1$	4.3901	-1.156	3.3384099	-3.44871	3.79	0.70
$\beta$ $C2/m$	4.6246	-1.282	3.6202172	-3.64241	3.97	1.01
$\gamma$ R-3m	0.7181	0.751	3.9521071	4.28401	-1.40	0.001

<sup>a</sup> Sum of squared differences between calculated and fitted data.

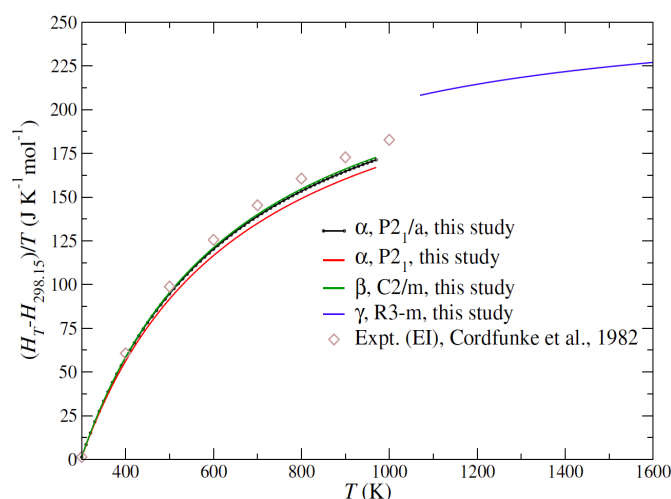


**Figure 5.** Thermal evolution of the enthalpy function of  $\alpha$ - $\text{Na}_2\text{U}_2\text{O}_7$  ( $P2_1/a$  and  $P2_1$ ),  $\beta$ - $\text{Na}_2\text{U}_2\text{O}_7$  ( $C2/m$ ), and  $\gamma$ - $\text{Na}_2\text{U}_2\text{O}_7$  (R-3m) computed with DFPT at the GGA/PBE level. The experimental values derived by Cordfunke et al. (1982) from enthalpy increments (EI) are also represented for comparison.

By analytical integration of the fit to the isobaric heat capacity, the enthalpy function was calculated according to:

$$(H_T - H_{298.15}) \cdot T^{-1} = \int_{298.15}^T (a + bT + cT^{-2} + dT^{-0.5} + eT^2) dT.$$

Results are displayed in Figure 5 for  $\alpha$ - $\text{Na}_2\text{U}_2\text{O}_7$  ( $P2_1/a$ ),  $\beta$ - $\text{Na}_2\text{U}_2\text{O}_7$  ( $C2/m$ ), and  $\gamma$ - $\text{Na}_2\text{U}_2\text{O}_7$  (R-3m). Calculations for  $P2_1/a$   $\alpha$ - and  $\beta$ -polymorphs are in overall good agreement with experimental values derived from EI by Cordfunke et al.<sup>16</sup>. At 900 K, i.e., in the vicinity of the stability limit of  $\beta$ - $\text{Na}_2\text{U}_2\text{O}_7$ , the experimental value of 172.76 J K<sup>-1</sup> mol<sup>-1</sup> is close to the DFPT predictions of

166.08 J K<sup>-1</sup> mol<sup>-1</sup> for  $\beta$ -phase (-3.9%). Although  $P2_1/a$   $\alpha$ -Na<sub>2</sub>U<sub>2</sub>O<sub>7</sub> might already have decomposed by 900 K, its calculated enthalpy function value at this temperature is 164.73 J K<sup>-1</sup> mol<sup>-1</sup>, ~4.6% smaller than experiment. The calculated enthalpy function for  $\gamma$ -Na<sub>2</sub>U<sub>2</sub>O<sub>7</sub> ranges from 208.21 and 227.44 J K<sup>-1</sup> mol<sup>-1</sup> between 1070 and 1620 K, where this phase was observed to be stable.

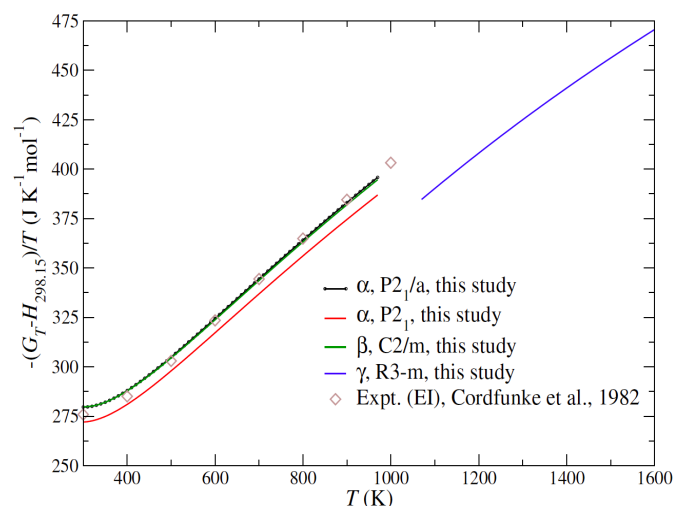


**Figure 6.** Thermal evolution of Gibbs energy function of  $\alpha$ -Na<sub>2</sub>U<sub>2</sub>O<sub>7</sub> ( $P2_1/a$  and  $P2_1$ ),  $\beta$ -Na<sub>2</sub>U<sub>2</sub>O<sub>7</sub> ( $C2/m$ ), and  $\gamma$ -Na<sub>2</sub>U<sub>2</sub>O<sub>7</sub> ( $R-3m$ ) computed with DFPT at the GGA/PBE level. The experimental values derived by Cordfunke et al. (1982) from enthalpy increments (EI) are also represented for comparison.

The Gibbs energy function was obtained using the following formula:

$$-(G_T - H_{298.15}) \cdot T^{-1} = S(T) - (H_T - H_{298.15}) \cdot T^{-1},$$

where  $S(T)$  is the entropy from DFPT calculations. As depicted in Figure 6, at room temperature the experimental value of the Gibbs energy function of 275.87 J K<sup>-1</sup> mol<sup>-1</sup> is well reproduced by DFPT calculations, with estimates of 279.63 J K<sup>-1</sup> mol<sup>-1</sup> for  $P2_1/a$   $\alpha$ -Na<sub>2</sub>U<sub>2</sub>O<sub>7</sub> (+1.3%) and 279.82 J K<sup>-1</sup> mol<sup>-1</sup> for  $\beta$ -Na<sub>2</sub>U<sub>2</sub>O<sub>7</sub> (+1.4%), while the value of 272.6 J K<sup>-1</sup> mol<sup>-1</sup> for  $P2_1$   $\alpha$ -Na<sub>2</sub>U<sub>2</sub>O<sub>7</sub> underestimates experiment by 1.4%. At 900 K, the experimental estimate of 384.49 J K<sup>-1</sup> mol<sup>-1</sup> is slightly larger than the predicted values of 383.06 J K<sup>-1</sup> mol<sup>-1</sup> for  $P2_1/a$   $\alpha$ -Na<sub>2</sub>U<sub>2</sub>O<sub>7</sub> (-0.4%), 381.95 J K<sup>-1</sup> mol<sup>-1</sup> for  $\beta$ -Na<sub>2</sub>U<sub>2</sub>O<sub>7</sub> (-0.7%), and 374.52 J K<sup>-1</sup> mol<sup>-1</sup> for  $P2_1$   $\alpha$ -Na<sub>2</sub>U<sub>2</sub>O<sub>7</sub> (-2.6%). The calculated Gibbs energy function for  $\gamma$ -Na<sub>2</sub>U<sub>2</sub>O<sub>7</sub> varies in the 1070-1620 K temperature range from 384.66 to 473.39 J K<sup>-1</sup> mol<sup>-1</sup>.

## Conclusions

In summary, polymorphism and phase transitions in Na<sub>2</sub>U<sub>2</sub>O<sub>7</sub> were investigated within the framework of DFT/DFPT to assess available structural and thermodynamic data, resolve issues on polymorph structures and relative thermal stability existing in the literature, and provide for the first-time thermodynamic functions for the high-temperature  $\gamma$ -Na<sub>2</sub>U<sub>2</sub>O<sub>7</sub> phase.

The present Gibbs free energy calculations show that  $\alpha$ -Na<sub>2</sub>U<sub>2</sub>O<sub>7</sub> ( $P2_1/a$ ) and  $\beta$ -Na<sub>2</sub>U<sub>2</sub>O<sub>7</sub> ( $C2/m$ ) are essentially

degenerate in energy at low temperature, with  $\beta$ -Na<sub>2</sub>U<sub>2</sub>O<sub>7</sub> becoming slightly more stable than  $\alpha$ -Na<sub>2</sub>U<sub>2</sub>O<sub>7</sub> as temperature increases. These findings corroborate XRD data showing a mixture of  $\alpha$  and  $\beta$  phases after cooling of  $\gamma$ -Na<sub>2</sub>U<sub>2</sub>O<sub>7</sub> to room temperature and the observation of a sluggish  $\alpha \rightarrow \beta$  phase transition above ~600 K. In addition, Gibbs free energy results demonstrate that the recently observed  $\alpha$ -Na<sub>2</sub>U<sub>2</sub>O<sub>7</sub> structure crystallizing in the  $P2_1$  space group is metastable at low temperature. At high temperature, DFPT calculations disprove the occurrence of a direct  $\beta \rightarrow \gamma$  solid-solid phase transition reported in some experiments at ~1348 K, but support instead the multi-step process consisting of  $\beta$ -phase decomposition into NaUO<sub>3</sub>(cr) and 1/2 O<sub>2</sub>(g), followed by recrystallization of NaUO<sub>3</sub> into  $\gamma$ -Na<sub>2</sub>U<sub>2</sub>O<sub>7</sub> and UO<sub>2</sub> at higher temperature, as proposed in recent experiments.

Phonon calculations conducted within the quasi-harmonic approximation yield standard molar isochoric heat capacity values of  $C_{p^0}(298.15 \text{ K}) = 219.4$  and  $220.9 \text{ J K}^{-1} \text{ mol}^{-1}$  for  $P2_1/a$   $\alpha$ -Na<sub>2</sub>U<sub>2</sub>O<sub>7</sub> and  $C2/m$   $\beta$ -Na<sub>2</sub>U<sub>2</sub>O<sub>7</sub>, respectively, i.e., 3.4 and 2.8% smaller than the experimental value of 227.26 J K<sup>-1</sup> mol<sup>-1</sup> measured by adiabatic calorimetry. The predicted standard molar entropy values are 279.6 J K<sup>-1</sup> mol<sup>-1</sup> for  $P2_1/a$   $\alpha$ -Na<sub>2</sub>U<sub>2</sub>O<sub>7</sub> and 279.8 J K<sup>-1</sup> mol<sup>-1</sup> for  $\beta$ -Na<sub>2</sub>U<sub>2</sub>O<sub>7</sub>, i.e., 1.3 and 1.4% larger than the experimental reference standard molar entropy  $S^0 = 275.86 \text{ J K}^{-1} \text{ mol}^{-1}$  derived by Cordfunke et al. from AC measurements. The thermal evolution of molar entropy predicted in this study up to ~1600 K for  $\gamma$ -Na<sub>2</sub>U<sub>2</sub>O<sub>7</sub> does not show any significant discontinuity with thermal variations calculated for  $\alpha$ - and  $\beta$ -Na<sub>2</sub>U<sub>2</sub>O<sub>7</sub> at lower temperature. Calculations of the enthalpy function and Gibbs energy function for  $P2_1/a$   $\alpha$ - and  $\beta$ -polymorphs are in overall very good agreement with experimental values derived from enthalpy increments by Cordfunke and coworkers. At 900 K, i.e., in the vicinity of the stability limit of  $\beta$ -Na<sub>2</sub>U<sub>2</sub>O<sub>7</sub>, the experimental value of 172.76 J K<sup>-1</sup> mol<sup>-1</sup> is close to the DFPT predictions of 166.08 J K<sup>-1</sup> mol<sup>-1</sup> for  $\beta$ -phase (-3.9%). The calculated enthalpy function for  $\gamma$ -Na<sub>2</sub>U<sub>2</sub>O<sub>7</sub> ranges from 208.21 and 227.44 J K<sup>-1</sup> mol<sup>-1</sup> between 1070 and 1620 K, where this phase was observed to be stable. The experimental value of the standard Gibbs energy function of 275.87 J K<sup>-1</sup> mol<sup>-1</sup> is also well reproduced by DFPT calculations, with estimates of 279.63 J K<sup>-1</sup> mol<sup>-1</sup> for  $P2_1/a$   $\alpha$ -Na<sub>2</sub>U<sub>2</sub>O<sub>7</sub> (+1.3%) and 279.82 J K<sup>-1</sup> mol<sup>-1</sup> for  $\beta$ -Na<sub>2</sub>U<sub>2</sub>O<sub>7</sub> (+1.4%).

In light of these new first-principles results, experimental high-temperature calorimetry measurements are desirable to validate and better constrain the thermodynamic functions of the  $\gamma$ -Na<sub>2</sub>U<sub>2</sub>O<sub>7</sub> phase up to ~1600 K. Additional first-principles calculations using similar methodology are also necessary to investigate hydrated forms of Na<sub>2</sub>U<sub>2</sub>O<sub>7</sub>, similar to the mineral clarkeite, as well as the high-temperature decomposition reactions of  $\beta$ -Na<sub>2</sub>U<sub>2</sub>O<sub>7</sub> and NaUO<sub>3</sub>(cr).

## Acknowledgements

Sandia National Laboratories is a multi-mission laboratory managed and operated by National Technology and Engineering Solutions of Sandia, LLC., a wholly owned subsidiary of

Honeywell International, Inc., for the U.S. Department of Energy's (DOE) National Nuclear Security Administration under Contract DE-NA0003525. This work was supported by the Spent Fuel and Waste Science and Technology (SFWST) Campaign and the Nuclear Energy University Program (NEUP) of the U.S. DOE Office of Nuclear Energy (NE). The views expressed in the article

do not necessarily represent the views of the U.S. DOE or the United States Government.

## References

- <sup>1</sup> K. Maher, J. R. Bargar, G. E. Brown, Jr., *Inorg. Chem.*, 2013, **52**, 7, 3510.
- <sup>2</sup> R. J. Baker, *Coord. Chem. Rev.*, 2014, **266-267**, 123.
- <sup>3</sup> R. J. Finch, E. C. Buck, P. A. Finn, J. K. Bates, *Mat. Res. Soc. Symp. Proc.*, 1999, **556**, 431.
- <sup>4</sup> A. L. Smith, P. E. Raison, L. Martel, T. Charpentier, I. Farnan, D. Prieur, C. Hennig, A. C. Scheinost, R. J. M. Konings, A. K. Cheetham, *Inorg. Chem.*, 2014, **53**, 375.
- <sup>5</sup> D. J. W. Ijdo, S. Akerboom, A. Bontenbal, *J. Sol. State Chem.*, 2015, **221**, 1.
- <sup>6</sup> A. L. Smith, C. Gueneau, J.-L. Fleche, S. Chatain, O. Benes, R.J.M. Konings, *J. Chem. Thermodynamics*, 2017, **114**, 93.
- <sup>7</sup> R. F. Carlstrom, *Ion Exchange Flowsheet for Recovery of Cesium From PUREX Sludge Supernatant at B Plant*. ARH-F-106. Atlantic Richfield Hanford Company, Richland, WA, 2017.
- <sup>8</sup> W. D. King, T. B. Edwards, D. T. Hobbs, W. R. Wilmarth, *Sep. Sci. Technol.*, 2010, **45**, 1793.
- <sup>9</sup> R. J. Finch, R. C. Ewing, *American Mineralogist*, 1997, **82**, 607.
- <sup>10</sup> D. E. Giammar, J. E. Hering, *Environ. Sci. Technol.*, 2004, **38**, 171.
- <sup>11</sup> C. Keller, C. Keller. Ed., *Gmelin Handbuch der Anorganischen Chemie, Uran*, No.55, Springer Verlag, Berlin, 1975.
- <sup>12</sup> L. M. Kovba, Y. P. Simanov, E. A. Ippolitova, V. J. Spitsyn, *Doklady Akademii Nauk SSSR*, 1958, **120**, 1042.
- <sup>13</sup> W. T. Carnall, A. Walker, S. J. Neufeldt, *Inorg. Chem.*, 1966, **5**, 2135.
- <sup>14</sup> E. H. P. Cordfunke, B. O. Loopstra, *J. Inorg. Nucl. Chem.*, 1971, **33**, 2427.
- <sup>15</sup> M. Gasperin, M., *J. Less-Common Met.*, 1986, **119**, 83.
- <sup>16</sup> E. H. P. Cordfunke, R. P. Muis, W. Ouweltjes, H. E. Flotow, P. A. G. Ohare, *J. Chem. Thermodyn.*, 1982, **14**, 313.
- <sup>17</sup> L. M. Kovba, *Sov. Radiochem. Engl. Trans.*, 1972, **14**, 746.
- <sup>18</sup> M.-C. Saine, *J. Less-Common Met.*, 1989, **154**, 361.
- <sup>19</sup> A. L. Smith, P. E. Raison, R. J. M. Konings, *J. Nucl. Mater.*, 2011, **413**, 114.
- <sup>20</sup> A. L. Smith, J. Y. Colle, P. E. Raison, O. Benes, R. J. M. Konings, *J. Chem. Thermodynamics*, 2015, **90**, 199.
- <sup>21</sup> G. Kresse, J. Furthmüller, *Phys. Rev. B*, 1996, **54**, 11169.
- <sup>22</sup> J. P. Perdew, J. A. Chevary, S. H. Vosko, K. A. Jackson, M. R. Pederson, D. J. Singh, C. Fiolhais, *Phys. Rev. B*, 1992, **46**, 6671.
- <sup>23</sup> J. P. Perdew, K. Burke, M. Ernzerhof, *Phys. Rev. Lett.*, 1996, **77**, 3865.
- <sup>24</sup> P. F. Weck, E. Kim, N. Balakrishnan, F. Poineau, C. B. Yeaman, K. R. Czerwinski, *Chem. Phys. Lett.*, 2007, **443**, 82.
- <sup>25</sup> P. F. Weck, E. Kim, B. Masci, P. Thuery, K. R. Czerwinski, *Inorg. Chem.*, 2010, **49**, 1465.
- <sup>26</sup> P. F. Weck, C.-M. S. Gong, E. Kim, P. Thuery, K. R. Czerwinski, *Dalton Trans.*, 2011, **40**, 6007.
- <sup>27</sup> P. F. Weck, E. Kim, C. F. Jové-Colón, D. C. Sassani, *Dalton Trans.*, 2013, **41**, 4570.
- <sup>28</sup> P. F. Weck, E. Kim, *Dalton Trans.*, 2014, **43**, 17191.
- <sup>29</sup> P. F. Weck, E. Kim, E. C. Buck, *RSC Advances*, 2015, **5**, 79090.
- <sup>30</sup> P. F. Weck, E. Kim, *J. Phys. Chem. C*, 2016, **120**, 16553.
- <sup>31</sup> P. F. Weck, C.F. Jové-Colón and E. Kim, *Phys. Chem. Chem. Phys.*, 2019, **21**, 25569.
- <sup>32</sup> P. F. Weck, C.F. Jové-Colón and E. Kim, *Chem. Phys. Lett.*, 2020, **757**, 137878.
- <sup>33</sup> P. E. Blöchl, *Phys. Rev. B*, 1994, **50**, 17953.
- <sup>34</sup> G. Kresse, D. Joubert, *Phys. Rev. B*, 1999, **59**, 1758.
- <sup>35</sup> E. R. Davidson, *Methods in Computational Molecular Physics*, G. H. F. Diercksen and S. Wilson, Eds., Vol. 113, NATO Advanced Study Institute, Series C, Plenum, New York, 1983, p. 95.
- <sup>36</sup> H. J. Monkhorst, J. D. Pack, *Phys. Rev. B*, 1976, **13**, 5188.
- <sup>37</sup> A. Togo, F. Oba, I. Tanaka, *Phys. Rev. B*, 2008, **78**, 134106.
- <sup>38</sup> I. Grenthe, J. Fuger, R.J.M. Konings, R.J. Lemire, A.B. Muller, C. Nguyen-Trung Cregu, H. Wanner. *Chemical Thermodynamics of Uranium*, OECD Nuclear Energy Agency, Data Bank, Issy-les-Moulineaux (France), 1992.